Correlating Interlayer Spacing and Separation Capability of Graphene Oxide Membranes in Organic Solvents

Submitted to

ACS Nano

02/20/2020

Sunxiang Zheng[a], Qingsong Tu[a#], Monong Wang[a], Jeffrey J. Urban[b], Baoxia Mi[a*]

[a] Department of Civil and Environmental Engineering
University of California
Berkeley, CA 94720

[b] The Molecular Foundry
Lawrence Berkeley National Laboratory
Berkeley, CA 94720

[*] The author to whom correspondence should be addressed. E-mail: mib@berkeley.edu; Tel.: (510) 664-7446
Co-first author

GRAPHIC ABSTRACT

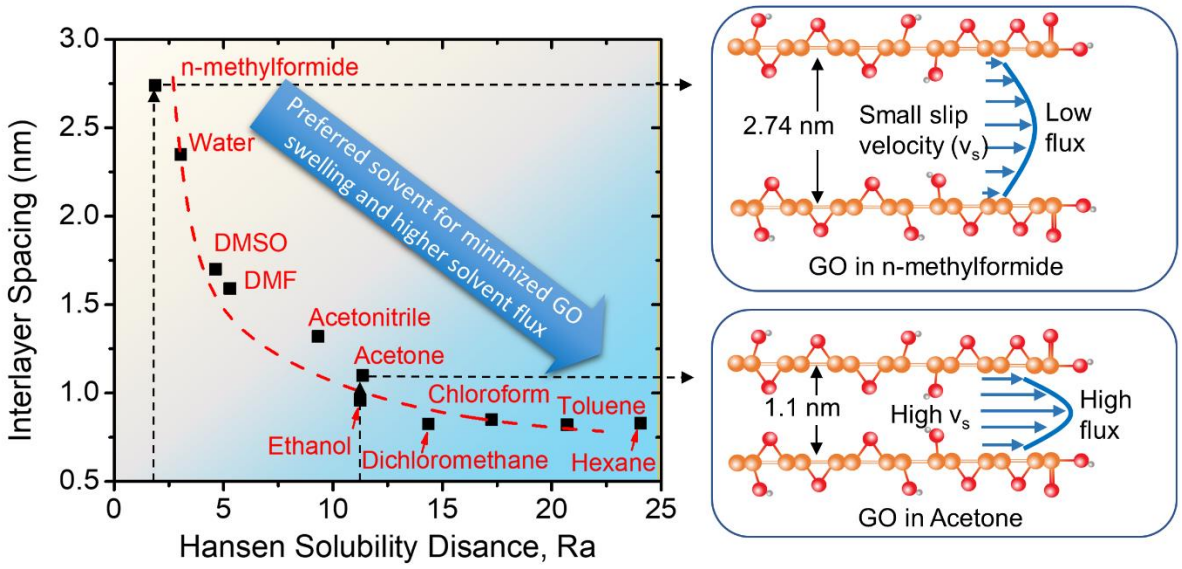

ABSTRACT

Membranes synthesized by stacking two-dimensional (2D) graphene oxide (GO) hold great promises for improved permeability and separation capability in organic solvents. However, the separation capability of a layer-stacked GO membrane in organic solvents can be significantly affected by its swelling and interlayer spacing, which has not yet been systematically characterized. In this study, the interlayer spacing of a layer-stacked GO membrane in different organic solvents was experimentally characterized by liquid-phase ellipsometry. To understand the swelling mechanism, the solubility parameters of GO were experimentally determined and used to mathematically predict the Hansen solubility distance (Ra) between GO and solvents, which is found to be a good predictor for GO swelling and the interlayer spacing. Solvents with low solubility distance (e.g., dimethylformamide, n-methyl-2-pyrrolidone) tend to cause significant GO swelling, resulting in an interlayer spacing of up to 2.7 nm. Solvents with high solubility distance (above 10) such as ethanol, acetone, hexane and toluene only cause minor swelling and are thus able to maintain an interlayer spacing of around 1 nm. Correspondingly, GO membranes in solvents with high solubility distance exhibit better separation performance, for example, more than 90% rejection of small organic dye molecules (e.g., rhodamine B and methylene blue) in ethanol and acetone. Additionally, solvents with higher solubility distance results in a higher slip velocity in GO channels and thus higher solvent flux through the GO membrane.

Keywords: Graphene oxide; Membrane; Interlayer spacing; Swelling; Solubility difference; Organic solvent nanofiltration.

Due to the intriguing mass transport phenomena in the confined channels, layer-stacked two-dimensional (2D) graphene oxide (GO) thin film has been intensively studied as a selective transport barrier in many important applications including gas separation, [1, 2] water purification,[3, 4] supercapacitors,[5] and batteries.[6] The surface of GO consisting of continuous hexagonal carbon lattice is considered impermeable to even the smallest molecules such as H_2 and H_2O,[7] while the nanosized channels formed naturally by self-stacking between two adjacent GO layers provide pathways for selective mass transport.[8] Since GO has excellent chemical stability in organic solvents, it has great potential to make selective membranes for separation in organic solvents such as acetone, dimethylformamide (DMF), and hexane that are frequently used in the petrochemical, food processing and pharmaceutical industries.[9] Analogous to aqueous phase separation, the interlayer spacing of the stacked GO layers in organic solvents, which is defined as the center-to-center distance of two adjacent carbon lattice is essential for the targeted performance of the layer-stacked GO membranes.[10, 11] However, most of the current studies on the interlayer spacing of GO membranes and the mass transport mechanisms through a GO membrane are limited to the gaseous and aqueous phase separation. Therefore, much work is needed for the fundamental understanding of the interlayer spacing of GO membranes in organic solvents.

The interlayer spacing of GO in liquid solvents was conventionally measured using X-ray Diffraction (XRD). However, sophisticated sample preparation is often required, as the presence of bulk liquid is usually not compatible with such a technique. Instead of directly characterizing the interlayer spacing, attempts have been made to measure the total thickness change of GO film after soaking it in bulk liquid, assuming the isotropic increase of interlayer spacing in the vertical direction is proportional to the total thickness change. For example, a pressurized contact thickness gauge was used to measure the swelling of GO membrane in a desalination system,[12] and liquid phase ellipsometry was applied to accurately characterize the swelling of GO in aqueous solutions. [13] While such techniques can be adapted to measure GO swelling in organic solvents, no systematic measurement has been reported to the best of our knowledge.

The interlayer spacing of GO film in the dry conditions was reported to be around 0.7 nm,[7, 14] which if stay unchanged is ideal to screen out molecules that present the most challenges in the organic solvent separation processes (200~1000 Da).[15] However, upon soaking in the liquid environment, solvent molecules could potentially cause swelling of GO layers,[16] resulting in compromised rejection performance. Taking the example of GO membranes in aqueous phase

separation, the swelling of GO membranes is severe due to the high affinity between water molecules and the polar functional groups on the GO surface,[17, 18] resulting in deteriorated selectivity.[19] The distance between two adjacent GO layers, without crosslinking, could increase to up to 6-7 nm in pure water and around 2 nm in salty water.[13] Such severe swelling can be attributed to strong hydration force at short distance and electrostatic repulsion force at long distance between two adjacent GO layers.[20, 21] However, our knowledge on GO swelling in aqueous solutions might not be applicable to organic solvents, because the electrostatic interactions between GO layers become much weaker and almost negligible in many organic solvents. That is why some non-polar organic solvents such as hexane and toluene are less likely to cause dramatic swelling of GO layers because of their low affinity to the GO surface.[22] Therefore, GO membranes could exhibit completely different swelling behavior and separation performance in different organic solvents, and work is needed to achieve the fundamental understanding and theoretical quantification of interlayer spacing of GO layers in organic solvents.

In addition, the transport of organic solvents in the confined 2D GO nanochannels may exhibit unique properties, which cannot be observed in the bulk.[23-25] For example, water molecules can form high-density (~ 1.3 g/cm^3), well-aligned water network in 2D GO channels that was theoretically predicted and experimentally detected in our previous study.[13] Such unique water structure induced by van der Waals (vdW) interactions between the graphitic regions of GO and water molecules potentially promotes fast water transport through the GO membrane.[26] Similarly, a recent theoretical study also predicts an enhanced transport of organic solvents in 2D GO nanochannels due to the fast slippage of solvent molecules on graphene surface.[27] Therefore, the interactions between solvent molecules and GO surfaces can affect the slip velocity and thus permeability of solvent through GO membranes. Such effects need to be well understood and quantified in order to systematically optimize layer-stacked GO membranes for best separation performance in organic solvents.

To fulfill these knowledge gaps, this study characterized the interlayer spacing of GO layers in organic solvents using a liquid-phase ellipsometer. To understand the swelling behavior, regular solution theory was adopted to describe the swelling based on the solubility of GO in organic solvents. The performance of GO membranes in organic solvents are tested in a pressurized nanofiltration membrane system. Molecular dynamics (MD) simulations were carried out to fundamentally understand solvent transport mechanisms in 2D GO nanochannels.

RESULTS AND DISCUSSION

Physiochemical Properties of GO Membranes

The GO nanosheets used to prepare GO membranes were synthesized using modified Hummer's method.[3] The lateral size of the synthesized GO nanosheets was measured to be around 800 nm using dynamic light scattering (Figure. S1). Some small GO nanosheets with lateral size down to 100 nm were also observed in AFM images (Figure 1A). The depth profile of AFM images of GO nanosheets shows that the GO nanosheets are mostly monolayers with a thickness around 1 nm. The degree of GO oxidation greatly affects the surface properties (e.g., wettability and surface charge) and potentially the interlayer spacing of GO in organic solvents. Therefore, the GO oxidation was characterized by XPS spectroscopy. As shown in Figure S2, the GO nanosheets are highly oxidized after chemical oxidation and ultrasonic exfoliation, exhibiting an O/C ratio of around 0.4. Figure 1B shows that around 45% of the carbon atoms on GO remain unoxidized, and the other 55% carbon atoms are associated with oxygenated functional groups such as hydroxyl, epoxide and carboxylic groups. The presence of ionizable oxygenated functional groups on GO nanosheets makes GO negatively charged in aqueous solutions with pH greater than 4 (Figure S3). The negative charge is known to play a very important role in increasing membrane hydrophilicity and selectivity due to electrostatic effects in aqueous phase environment.[28]

However, the charge properties of GO are very different in organic solvents. The dissociation of oxygenated functional groups in organic solvent is greatly suppressed due to relatively poor proton transfer capability.[29] For example, it has been reported that the pKa of carboxylic groups, which serve as the main source of the negative charges on GO, increases drastically in organic solvents.[30] Such pKa shift is linearly proportional to the inverse of dielectric constant of the organic solvent according to Born's theory of ionic solvation.[31] The dielectric constant of most organic solvents is lower than that of water. Therefore, GO in organic solvents tends to exhibit neutral or weak negative charges. As confirmed by the charge measurements in Figure S4, the zeta potential of GO in organic solvents such as ethanol and hexane are in the range of -10 mV to 0 mV, much weaker than the zeta potential of -40 mV in water.

In addition to surface charge, the wettability of GO membranes in organic solvents also plays an important role in determining membrane performance, such as solvent permeability.[32] Typically, solvents would experience increased transport resistance at the liquid-solid interface for membranes that can be hardly wetted.[33] As shown in Figure S5, the wettability of GO can be

characterized by the contact angle of solvents on the GO membrane using a tensiometer. The equilibrium contact angle of nonpolar solvents like hexane and some polar solvents like ethanol and acetone are almost zero, and the highest contact angle (28°) was obtained in water. Figure 1C shows the Zisman plot of a typical GO membrane surface, from which the critical surface tension of GO surface was calculated to be 39 mN/m. Therefore, solvents that have surface tension lower than 39 mN/m are expected to completely wet the membrane surface with negligible interfacial transport resistance. The observed good wettability thus indicates the potential of achieving high solvent flux.

Before making the layer-stacked GO membrane, GO suspension was sonicated and centrifuged to ensure a uniform dispersion of GO monolayer nanosheets. The GO nanosheets were then deposited on a Nylon membrane support by vacuum filtration to form a restacked GO membrane. As shown in Figure 2D, the bare Nylon substrate has interconnected pores with diameter of around 0.2 μm, which is considered incapable of rejecting small organic molecules. After the GO deposition, a continuous, smooth film was formed with a thickness of around 300 nm (Figure 1E and 1F), completely blocking the large pores in Nylon. As a result, the separation capability of the membrane would be governed by the structure and properties of the layer-stacked GO film.

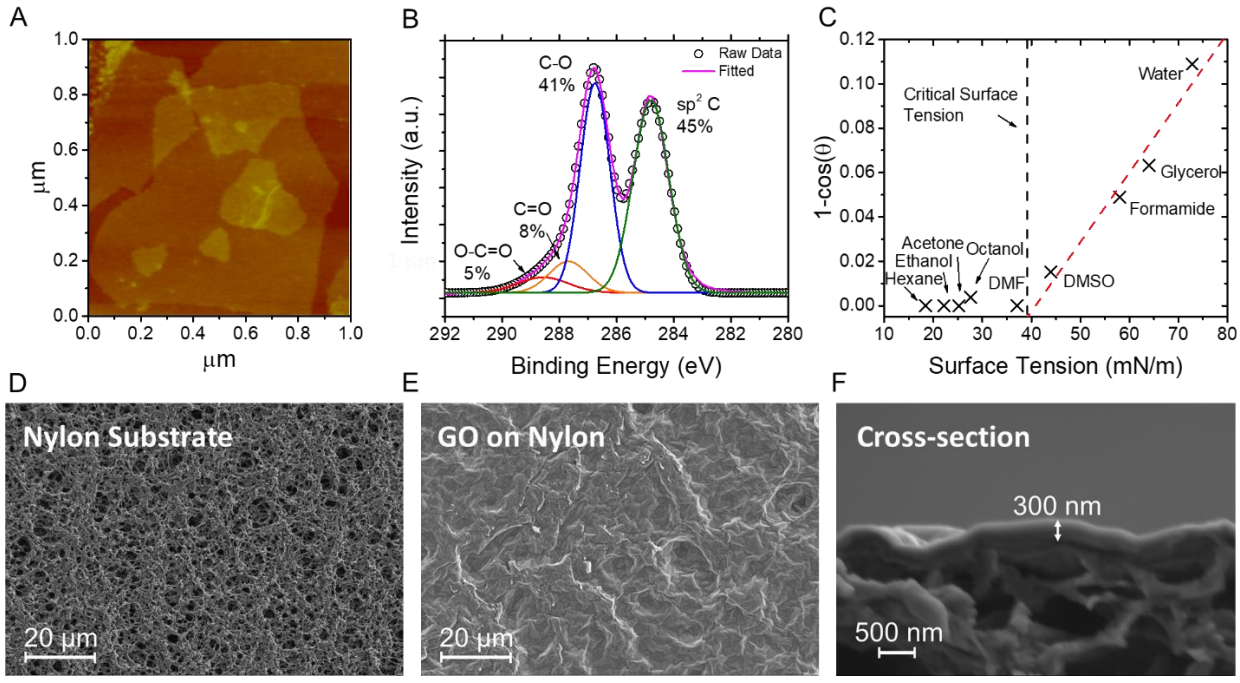

Figure 1. Physicochemical properties of GO nanosheets and layer-stacked GO membranes. AFM image of the as-synthesized GO nanosheets with a depth profile analysis demonstrating a monolayer thickness of around 1 nm (A). XPS characterization of the as-synthesized GO confirming the abundance of oxygenated functional groups (B). The Zisman plot to extrapolate the critical surface tension of GO (C). The SEM images of the Nylon substrate (D), the top surface of GO membrane (E), and the GO membrane cross section (F). DMSO and DMF refer to dimethyl sulfoxide and n,n-dimethylformamide, respectively.

Characterization of Interlayer Spacing by XRD and Liquid-Phase Ellipsometry

The interlayer spacing of layer-stacked GO in dry condition can be conveniently characterized by XRD.[16, 34] Before oxidation, graphite has an interlayer spacing of 0.34 nm,[35] which is almost the van de waals thickness of a single layer of carbon atoms.[36] Because of the presence of oxygenated functional groups protruding from the carbon lattice, the interlayer spacing of GO increases to 0.78 nm. After submerging in organic solvents, the interlayer spacing of GO may further expand due to the intrusion of solvent molecules into the channels between GO nanosheets, resulting in GO membrane swelling. To quantify the swelling, XRD can be used to characterize a GO membrane after soaking it in organic solvents for 24 hours to equilibrate. Figure 2A shows the shift of XRD peak from an interlayer spacing of 0.78 nm in initial dry state to 0.82-1.2 nm in selected organic solvents. The results agree well with previously reported values.[37] The GO membrane does not swell much in non-polar solvents, such as hexane and toluene, but it does swell dramatically in polar solvents, such as acetonitrile. Note that acquiring repeatable XRD data becomes extremely challenging when the GO swelling goes beyond a threshold.

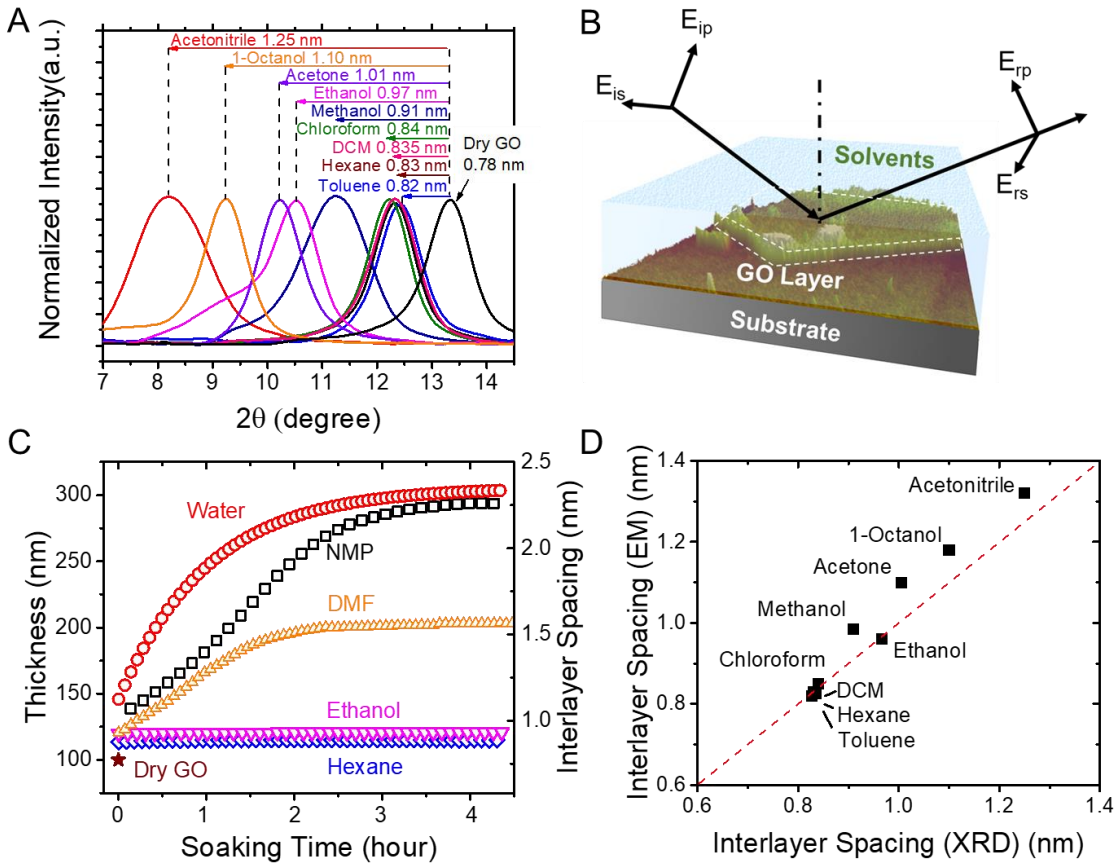

Figure 2. Characterization of the interlayer spacing of GO membranes in organic solvents. The XRD measurements of interlayer spacing of GO membranes after being soaked in various solvents (A). Schematic illustration of the liquid-phase ellipsometry as an alternative method to characterize the interlayer spacing of GO while being soaked in solvents. The measurement is an optical approach based on the polarization from incident light E_{is} and E_{ip} to reflected light E_{rs} and E_{rp} (B). The kinetics of GO swelling in selected solvents characterized by the liquid-phase ellipsometer (C). The comparison of interlayer spacing obtained from ellipsometer (EM) and XRD (D). DCM, NMP, and DMF refers to dichloromethane, n-methyl-2-pyrrolidone, and n,n-dimethylformamide , respectively.

For solvents that cause more significant GO swelling and result in an interlayer spacing that is too large for XRD to measure, liquid-phase ellipsometry offers an alternative approach. In addition, ellipsometry can measure the interlayer spacing while the sample is submerged in solvents, while XRD requires the sample to be taken out from the solvent before measurements. To prepare for a swelling test using ellipsometry, a 100 nm thick GO membrane was deposited on

a substrate via a transplanting method described in our previous study (Figure 2B).[38] The GO coated substrate was then mounted in a customized cell with side windows that allow light to go through. During measurements, two incoming perpendicular light waves E_{ip} and E_{is} shine on the GO membrane and polarize into E_{rp} and E_{rs} while being reflected to a detector. The GO membrane thickness can be monitored in-situ in the solvents and calculated using Cauchy equation that is described in SI and Figure S6. The average interlayer spacing of GO in the solvents ($d_{solvents-GO}$) was then calculated as

$$d_{solvents-GO} = d_{Dry-GO} \times \frac{\tau_{solvents-GO}}{\tau_{Dry-GO}} \quad (1)$$

where $\tau_{solvents-GO}$ and τ_{Dry-GO} are the total thickness of GO membrane in solvents and in dry state, respectively.

As shown in Figure 2C, the GO membrane does not swell at all while being soaked in ethanol and hexane for at least four hours. However, the thickness of GO increased dramatically within the first two hours of soaking in water, NMP and DMF, indicating fast swelling due to the adsorption of solvents into the GO layers. The swelling diminishes or becomes much slower after 4 hours. To examine the accuracy of ellipsometry measurements, we compared the interlayer spacing measured by ellipsometry to that by XRD. As shown Figure 2D, the two approaches generate very consistent interlayer spacing measurements. However, the interlayer spacing obtained by ellipsometry is consistently around 10% larger than that obtained by XRD. This is most likely because ellipsometry measures the average interlayer spacing of GO in a large area, while XRD only measures the interlayer spacing of well aligned regions.

Understanding the Interlayer Spacing of GO in Organic Solvents

The quantitative prediction of membrane swelling in organic solvents are challenging.[39, 40] It has been demonstrated that GO swelling in aqueous solutions can be well modeled by the Derjaguin-Landau-Verwey-Overbeek (DLVO) theory,[13] but such models might not be applicable for organic solvents due to the change in electrical double layer.[41, 42] In aqueous solutions, the interlayer spacing of GO layers is determined by the thickness of electrical double layer, defined as Debye length λ_D, which can be calculated as

$$\lambda_D = \sqrt{\frac{\varepsilon_S \varepsilon_0 kT}{2N_A e^2 I}} \quad (2)$$

where ε_s is the dielectric constant of a solution, ε_0 the vacuum permittivity, k the Boltzmann constant, T the absolute temperature; N_A the Avogadro number; e the electron charge, and I the ionic strength of the bulk solution. Using this model, the dielectric constant of a solution correlates well with the swelling degree of laminar structures.[43, 44] However, such linear correlation might not be true for organic solvents. Several studies reported that no swelling is observed when the dielectric constant is below a threshold, or in other cases, swelling reaches a plateau when the dielectric constant exceeds a certain value.[45, 46] We plotted the measured interlayer spacing of GO versus the dielectric constant of solvents in Figure S7 and observed relatively poor correlations. Therefore, an alternative model is needed to fully explain/predict GO swelling in organic solvents.

Ideas from the age-old saying "like dissolve like" indicates that GO swelling is likely to be strongly affected by its solubility in organic solvents. The solubility parameters and dipole moments of selected solvents are summarized in Table S1. We experimentally measured the solubility of GO in these solvents. As shown in Figure 3A, GO dissolves much better in polar solvents (e.g. DMF, NMP) than in nonpolar ones (e.g. hexane, toluene). Among the polar solvents, solvents with greater dipole moment (e.g., DMSO, DMF and NMP), i.e., stronger dipole-dipole intermolecular interactions, have higher GO solubility. It indicates that dipole-dipole interaction is a governing factor in determining GO solubility. In addition, the formation of hydrogen bond (H-bond) also contributes to the GO solubility in solvents. For instance, polar protic solvents like water and formamide can form strong H-bond with oxygenated functional groups on GO and result in high GO solubility. Polar aprotic solvents, such as DMSO, DMF, NMP and acetonitrile, can only be the acceptor of protons, thus having weaker capability of forming H-bond and dissolving GO. In non-polar solvents, GO barely dissolves because neither H-bond nor dipole-dipole interactions are present. The low solubility of GO in non-polar solvents also reveals that the dispersion cohesive interactions (non-polar interactions) are not capable of dissolving GO.

The measured solubility of GO in fifteen different solvents are plotted against the interlayer spacing of GO in each corresponding solvent in Figure 3B, and a strong correlation was observed. Solvents that can keep a large amount of GO nanosheets suspended result in larger interlayer spacing in a GO membrane. It indicates that the interlayer spacing of GO membrane may be potentially estimated based on the regular solution theory. The regular solution theory has been proved to predict the swelling of polymers in organic solvents surprisingly well, although some assumptions are made in the prediction.[47-49] It was also used to predict the swelling of layered

montmorillonite,[50] demonstrating the feasibility of describing the swelling of layer-stacked 2D nanomaterial using the solution theory.

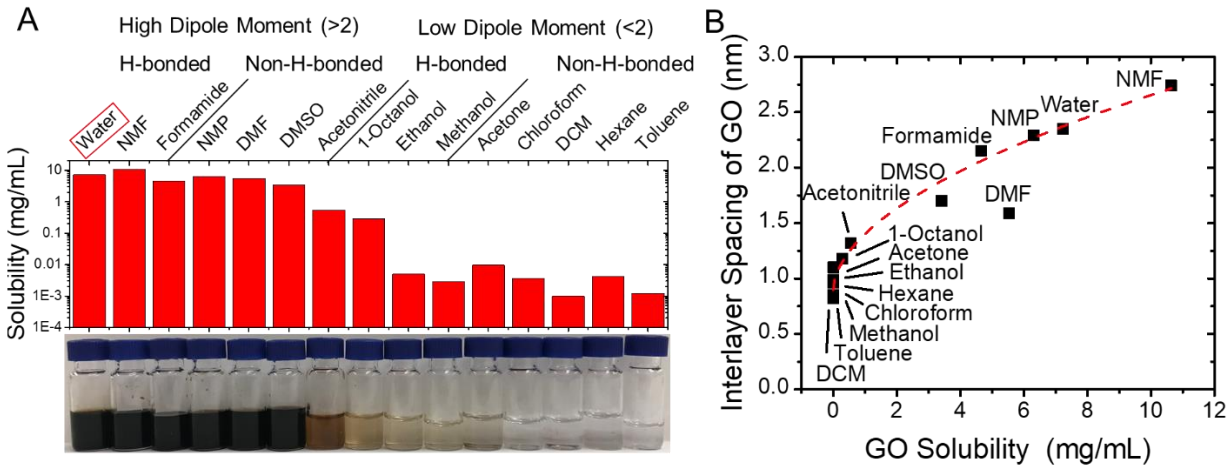

Figure 3. The experimentally measured solubility of GO in selected solvents (A), and its strong correlation with the interlayer spacing of GO obtained from ellipsometry measurements (B).

In order to develop a universal model to predict the swelling of GO in different solvents, we need to determine the solubility parameters of GO first. Based on the traditional dissolution theory developed by Hildebrand,[51] the molar energy change (ΔE) of mixing two components with negligible total volume change can be calculated as

$$\Delta E = V_m \alpha_1 \alpha_2 (\delta_1 - \delta_2)^2 \quad (3)$$

where α_1 and α_2 are the volume fractions of the two components, and δ_1 and δ_2 the Hildebrand solubility parameters of the two components. The Hildebrand solubility parameter (δ) is defined as

$$\delta = \left(\frac{\Delta_g U}{V_m}\right)^{1/2} \quad (4)$$

where $\Delta_g U$ is the energy required to vaporize one mole of the pure component, and V_m is the molar volume.

It is challenging to obtain the Hildebrand solubility parameter of GO, because unlike pure solvents, GO has no quantifiable vapor pressure, as needed in Equation 4. Therefore, we developed an alternative approach to estimate the solubility parameter of GO in this study. As suggested by Equation 3, the maximum solubility can be obtained when GO has similar solubility parameter to

the solvent, because when the Hildebrand solubility parameter of the two components are close to each other (i.e., $\delta_1 - \delta_2$ approaches zero), ΔE is minimized and the mixing of the two components results in the highest solubility. Figure 3B demonstrated that GO has the highest solubility in N-methlyformamide (NMF) among the fifteen representative solvents. It suggests that the Hildebrand solubility parameter of GO is close to that of NMF, which is around 30 $Mpa^{1/2}$.

However, the Hildebrand solubility parameter of GO alone is not a good predictor for GO swelling. As demonstrated in Figure 4A, although a good agreement (trend identified by the red dashed line) was observed for most solvents, there are a few outliers. In general, the interlayer spacing of GO has the largest value (~2.7 nm) in NMF and decreases considerably when the Hilderbrand solubility parameter deviates (increases or decreases) from 30 $Mpa^{1/2}$. The minimum swelling occurs in solvents with Hilderbrand solubility parameter deviating the most, i.e., in hexane or toluene with values going below 20 $Mpa^{1/2}$. However, in some solvents, such as ethanol and DMSO that have similar Hilderbrand solubility parameter (26.5 $Mpa^{1/2}$ vs. 26.7 $Mpa^{1/2}$) to that of GO (30 $Mpa^{1/2}$), very different swelling behavior was observed, for example, 0.96 nm interlayer spacing for ethanol and 1.7 nm for DMSO. This is most likely because multiple intermolecular interactions co-exist, and the single Hildebrand solubility parameter does not completely explain the swelling of GO.

To account for the different intermolecular interactions that contribute to the overall solubility and swelling of GO, the Hildebrand solubility parameter can be further split into the dispersion cohesive parameter δ_D, the polar cohesive parameter δ_P, and the H-bond parameter δ_H, which are known as the Hansen solubility parameters, as illustrated below

$$\delta^2 = {\delta_D}^2 + {\delta_P}^2 + {\delta_H}^2 \quad (5)$$

where the three Hansen solubility parameters δ_i of GO can be estimated by using the solubility-weighted average as illustrated in Equation 6.

$$\delta_{i,GO} = \frac{\sum S_{solvent}\delta_{i,solvent}}{\sum S_{solvent}} \quad (6)$$

where $S_{solvent}$ is the experimentally tested solubility of GO in a given solvent, and $\delta_{i,solvent}$ the Hansen solubility parameters for each solvent that are available in the literature.

Using Equation 6, the Hansen solubility parameters of GO, $\delta_{D,GO}$, $\delta_{P,GO}$, and $\delta_{H,GO}$, are calculated to be 17.5 $Mpa^{1/2}$, 19.1 $Mpa^{1/2}$, and 15.4 $Mpa^{1/2}$, respectively. Our results are in good consistence with the reported Hansen solubility parameters except that our δ_P value is higher than

the 10 $Mpa^{1/2}$ reported by Konios et al.[52] This discrepancy might be a result of the different oxidation degree of GO used in different studies. In Figure 4B, we illustrated the Hansen space created by the three-dimensional plots of δ_D, δ_P, and δ_H. The Hansen solubility parameters of GO determines the center (star symbol in Figure 4B) of a sphere, which is the so-called Hansen solubility sphere (pink sphere in Figure 4B). If a solvent is located within the sphere, it is a good solvent for dissolving GO (solubility > 0.5 mg/mL), and outside a bad solvent (solubility < 0.5 mg/mL). For visual convenience, the 3D Hansen space can also be translated into a two-dimensional plot (Figure S8), where we found the polar-polar interactions (high dipole and hydrogen bond) contribute the most to the solubility of GO, implying the importance of oxygenated functional groups to the solubility and swelling of GO in organic solvents.

In order to quantitatively use the Hansen solubility sphere, we defined a solubility distance (Ra) in the Hansen space. The Hansen solubility distance is calculated by the distance between the two points given by the solvent coordinates ($\delta_{\mathrm{D,solvent}}, \delta_{\mathrm{P,solvent}}, \delta_{\mathrm{H,solvent}}$) and the GO coordinates ($\delta_{\mathrm{D,GO}}, \delta_{\mathrm{P,GO}}, \delta_{\mathrm{H,GO}}$), as shown below

$$\mathrm{Ra}^2 = 4(\delta_{\mathrm{D,GO}} - \delta_{\mathrm{D,solvent}})^2 + (\delta_{\mathrm{P,GO}} - \delta_{\mathrm{P,solvent}})^2 + (\delta_{\mathrm{H,GO}} - \delta_{\mathrm{H,solvent}})^2 \quad (7)$$

The radius of the Hansen sphere is estimated to be ~ 9.5. It indicates that a solvent that has a Ra < 9.5, i.e., within 9.5 unit from the point of GO in the Hansen space could be considered a good solvent for GO.

The Hansen solubility distance (Ra) is plotted against the GO interlayer spacing in Figure 4C and it exhibits a clear correlation, which indicates that the interlayer spacing of GO follows an exponential decay with the increase of Ra, i.e., GO swells less with the increase of solubility distance. However, NMP seems to cause more dramatic swelling than predicted. This could be due to some other interactions beyond Hansen solubility parameters. Indeed, NMP contains lactam structure that was reported to have π- π interactions with the aromatic rings on GO.[53] Nevertheless, we found Hansen solubility distance (Ra) is so far the best predictor for GO swelling and the interlayer spacing of GO. Recently, some other 2D nanomaterials such as MoS_2 and MXene were also investigated as membranes in organic phase separation.[54, 55] Such method could potentially be universally applied to other emerging 2D nanomaterials to understand their solubility and swelling in organic solvents.

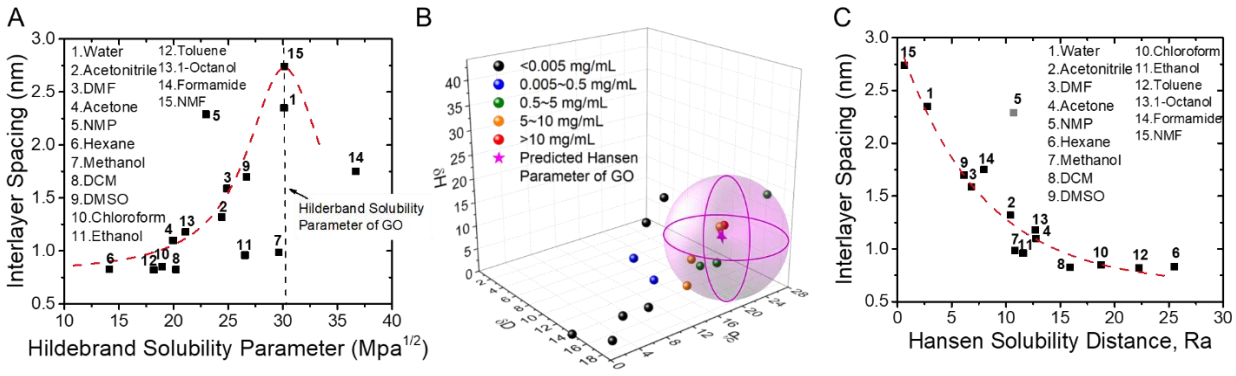

Figure 4. Prediction of GO swelling/the interlayer spacing of GO based on solubility parameters. Correlation between the interlayer spacing of GO and the Hildebrand solubility parameter (A). Illustration of Hansen space based on the Hansen solubility parameters of solvents and the predicted value for GO (B). Correlation between the interlayer spacing of GO and the solubility distance (Ra) in Hansen space (C).

Solvent Flux and Mass Transport Mechanisms in GO Membranes

The separation performance (i.e., solvent flux and solute rejection) of the layer-stacked GO membrane in organic solvents were tested in a pressurized nanofiltration system. The GO membranes were soaked in a solvent for at least 6 hours to reach an equilibrium interlayer spacing before each test. Despite of drastic swelling in some solvents, no delamination was observed during the soaking or testing, as confirmed by the pictures in Figure S9. For pressure-driven flow, solvent transport through two parallel GO nanosheets can be described by the Hagen-Poiseuille equation for viscous flow assuming a no-slip boundary condition:

$$J = \frac{d^4 \Delta P}{12 \eta W^2 L} \tag{8}$$

where the flux of the solvent J is a function of the distance between two plates d (i.e., the interlayer spacing of GO), the width of the plate W (i.e., lateral size of GO, ~800 nm), the total thickness of the GO membrane L (~300 nm), the applied pressure ΔP , and the viscosity of the solvents η.

Equation 8 describes a linear correlation between solvent permeability ($J/\Delta P$) and solvent-relevant parameters (d^4/η), as observed in Figure 4A. However, there should be only one slope in the linear relation because the slope only depends on the properties of GO, but we observed two drastically different slopes in Figure 4A. It appears that the solvents with high Hansen

solubility distance (Ra>9.5) exhibit low transport resistance that results in steeper slope, while the solvents with low Hansen solubility distance (Ra<9.5) exhibit higher transport resistance and thus smaller slope. This is most likely due to the difference in boundary slip velocity that is not described by Equation 8, which assumes a slip velocity of zero for all solvents. Large slip velocity has been reported for water transport in graphene channels, but the slip velocity and water flux decrease significantly when the graphene is decorated by oxygenated functional groups that induce strong interactions with water.[56] Similarly, for solvents with lower Hansen solubility distance, there are stronger interactions between solvents and GO to induce friction, thus the slip velocity would be smaller than that for solvents with higher Hansen solubility distance.

To verify our hypothesis, we conducted molecular dynamics simulation of solvent transport in confined GO nanochannels, which were described in detail in SI. As shown in Figure 5B, two GO nanosheets were constructed in parallel with an interlayer spacing of 3 nm. The GO nanosheets are decorated by oxygenated functional groups, with 20% being hydroxyl and 33% being epoxy as indicated by the XPS characterization (Figure 1B and S10). After introducing solvents into the system, the GO nanosheets are allowed to adjust the interlayer spacing to achieve a minimum system energy. A pressure gradient of 50 bar was applied along the GO nanochannel to drive the solvent transport. The velocity profile in Figure 5C exhibits a characteristic parabolic velocity distribution, with the slip velocity at the boundary being greater than zero. The simulation results in Figure 5C demonstrate that solvents that have high solubility distance (Ra), such as acetone and ethanol, have higher slip velocity and thus lower transport resistance and higher permeability than solvents with low Ra. In other words, when the solvent "dislikes" the GO nanosheets (i.e., large Ra), the permeability of the solvent in GO is higher.

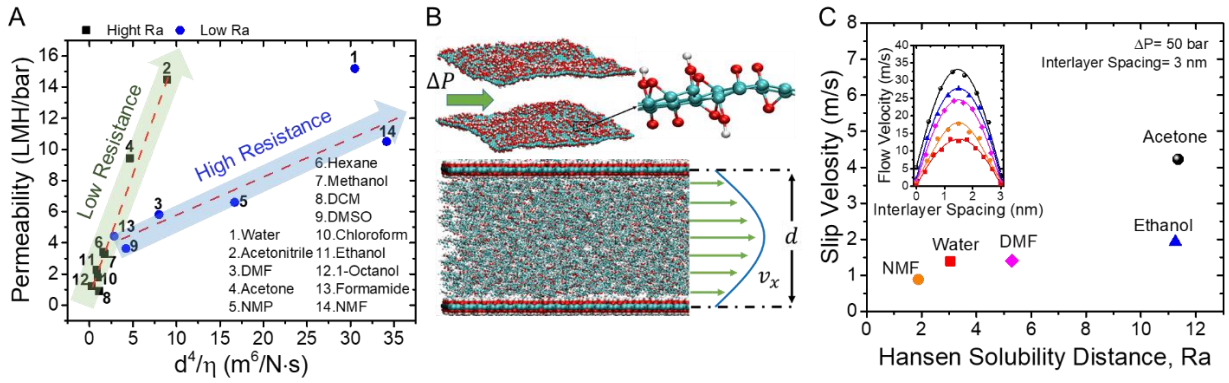

Figure 5. Solvent transport mechanisms in GO membrane. The effect of solvent properties (d^4/η) and Hansen solubility distance (*Ra*) on the permeability of solvents through GO membranes **(**A). Schematic illustration of molecular dynamics modeling of solvents transport in two parallel GO nanosheets with a trans-membrane pressure of ΔP (B). The interlayer spacing of the modelled GO nanosheets were fixed at 3 nm. The effects of Hansen solubility distance (solvent-GO likeness) on the slip velocity of selected solvents. The insertion illustrates the representative flow velocity profiles of different solvents in GO channels (C).

To understand the separation capability of GO membrane in different organic solvents, we tested the rejection of Rhodamine B (RB, MW 479 g/mol) and Methylene Blue (MB, MW 320 g/mol). As shown in Figure 6 A and B, the rejection of dyes dissolved in chloroform and DCM, which do not cause membrane swelling, can reach over 90%. The rejection decreases as the interlayer spacing increase due to GO swelling, indicating a strong correlation between the size of the GO nanochannel and the membrane separation capability. The solute separation by GO membranes in the aqueous system has been commonly attributed to three major mechanisms, including size exclusion, Donnan exclusion and hindered diffusion[57] In non-aqueous system, because the charges of both dye and GO are weak, size exclusion and hindered diffusion are believed to be the main separation mechanisms.

In addition, the relative affinity of dye molecules towards GO and solvents plays an important role in rejection. For example, the rejection of RB and MB in acetone is consistently higher than that in ethanol, although the GO membrane has slightly higher interlayer spacing in acetone (~1.1 nm) than that in ethanol (~0.96 nm). To understand the affinity, we measured the solubility of RB and MB in different organic solvents (Figure S11). If the affinity between the membrane and the dye molecules are greater than the affinity between the solvents and the dye molecules, the dye molecules tend to stay with the membrane and diffuse at a much slower rate than the solvent, resulting in higher rejection. Indeed, taking MB as an example, the solubility of MB in ethanol was measured to be 102 mg/mL (Figure S9), which is 1000 times greater than that in acetone, revealing a dramatically higher affinity between MB and ethanol than that between MB and acetone. As a result, MB is much easier to be carried by ethanol than by acetone through the GO membrane to the permeate side.

When the interlayer spacing of GO increases to over 2 nm, we observed less than 10% rejection of the dye in organic solvents since the size of the dye molecules is estimated to be around 1 nm. Interestingly, we found that the rejection of RB and MB in water is much higher (~40%) than that in organic. A plausible reason is that both RB and MB are positively charged in water with neutral pH, which can be electrostatically attracted to the negatively charged GO nanosheets. Such electrostatic attraction is considered stronger than the attractive π-π interaction at a large separation distance.

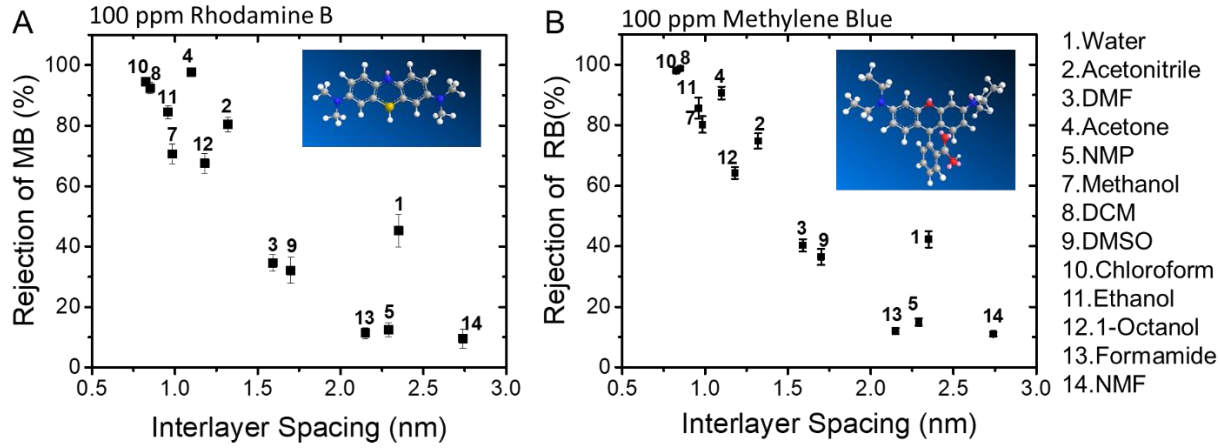

Figure 6. Rejection of methylene blue (A) and rhodamine B (B) by GO membranes in different organic solvents. Inserted are the chemical structures of methylene blue and rhodamine B.

Implication for GO Membrane Design and Application

The result of this study has significant implications for the GO membrane synthesis and applications in organic phase separation such as the emerging organic solvent nanofiltration (OSN). We have demonstrated that the GO membrane can have very different swelling behaviors in a variety of organic solvents and the equilibrium interlayer spacing can be predicted by Hansen solubility distance, Ra. The interlayer spacing of GO significantly affects the selectivity of the GO membranes. Therefore, for solvents that cause significant GO swelling, stabilizing method such as crosslinking need to be used. On the other hand, if the solvents are known to cause little swelling, stabilizing method might not be necessary for the sake of higher permeability and lower process cost. In addition, GO membrane has superior performance in some solvents such as acetone. We compared the membrane performance result of the present work with some other membranes in the literature (Table S2). The layer-stacked GO membrane has comparable separation capability in

acetone compared to some state-of-the-art OSN membranes, yet near 10 times higher permeability. Since acetone is an important solvent in the personal care and pharmaceutical industries, there is a great potential for GO membranes in these applications. Moreover, it has been revealed that the oxidation degree of GO affects its solubility parameter, and herein the swelling of GO in organic solvents. Therefore, performance of the GO membrane can potentially be fine tuned by careful control of the GO during synthesis or partial reduction. Recently, some other 2D nanomaterials such as MoS_2 and MXene were also investigated as membranes in OSN.

METHODS

Chemicals

All chemicals were used as received from Sigma-Aldrich (St. Louis, MO) unless noted otherwise. The chemicals used in the present study included H_2O_2, H_2SO_4, $NaNO_3$, Na_2SO_4, graphite, acetone, acetonitrile, ethanol, methanol, 1-ocatanol, hexane, toluene, chloroform, dichloromethane, n-methyl-2-pyrrolidone (NMP), n,n-dimethylformamide (DMF), dimethyl sulfoxide (DMSO), n-methylformamide (NMF), formamide, and rhodamine B. GO was prepared from graphite flakes using modified Hummers method with a detailed procedure described in our earlier publication.[3]

Characterization of GO Membrane

X-ray photoelectron spectroscopy (XPS, PHI 5400, Perkin-Elmer, Eden Prairie, MN) was used to characterize the elemental composition of GO. Atomic force microscope (AFM, Dimension Icon, Bruker, Santa Barbara, CA) images were taken to characterize the thickness and lateral dimension of GO monolayer deposited on a silicon wafer. The contact angle of solvents on the GO membrane surface were measured using an optical tensiometer (Theta Lite, Biolin Scientific, Sweden). Scanning electron microscopy (SEM, Ultra-55 FESEM, ZEISS) images were taken for the surface of the Nylon substrate before and after the GO coating. Cross-sectional images were obtained to evaluate the thickness of the GO coating. The zeta potential of GO sheets in the aqueous solutions were measured using a Zetasizer Nano-ZSP analyzer (Malvern, Westborough, MA). The interlayer spacing of GO in the dry state and solvents were characterized by X-ray diffraction (XRD, Bruker D8 Discover GADDS) with a graphite-monochromated Co Ka radiation (λ = 0.179 nm).

Interlayer Spacing Measurements via Liquid-phase-Ellipsometry

A multi-wavelength ellipsometer (FS-1Multi-wavelength, Film Sense, Lincoln, NE) was equipped with a cross-flow chamber (Biolin, Sweden), which allows the optical measurement through the two windows on each side of the chamber while maintaining a steady cross-flow through the chamber driving by a peristaltic pump. A gold-coated quartz disc (Biolin, Sweden) was used as the substrate for GO layers. The optical properties of the gold substrate in the dry state and in the solvents were first measured in the chamber as the baseline. Cross flow of the solvents was kept at 1 mL/min to mimic the fluid condition in a real filtration system. The GO water suspension was diluted and filtrated through a polyethersulfone (PES, Sterlitech, Kent, WA) membrane to form a 100 nm thick GO layer. To coat the GO, the gold substrate was placed upside down on the GO-coated PES membrane, with its top surface contacting the GO thin film. The GO film was then transplanted onto the gold substrate after peeling the disc off the membrane surface. The optical properties of the GO-coated substrate in the dry state and in the solvents were characterized using the ellipsometer. The ellipsometry data were analyzed by establishing an optical model. In general, data collected for the GO-coated substrate were fitted using Cauchy's equation to determine the film thickness in the dry state and in the solvents using the optical constants (i.e., refractive index and extinction index) of the solvent as the ambient parameters. More information about data analysis is provided in the SI.

GO Solubility in Solvents

Dry GO powder was first acquired by drying the GO water suspension in a freeze-dryier (FreeZone, Labconco). The GO power was collected and re-dissolve into various solvents. The concentration of GO in the solvents were determined by establishing calibration curves in the solvents. For instance, 1 mg GO powder was dissolve in 1 mL DMF and further diluted to obtain GO DMF-suspensions with a series of concentrations. The UV absorption of the GO in DMF at the characteristic peak of 350 nm was measured by a UV-vis spectrophotometer (Genesys 10S UV-Vis, Thermo fisher) and correlated with the mass concentration of GO. To measure the solubility of GO in the solvents, GO powder was overdosed in the solvents and mildly sonicated in a bath sonicator. The GO suspension in the solvents were subsequently centrifuged twice to remove excessive GO solids. The concentration of the supernatant was determined using the established calibration curve.

GO Membrane Preparation and Performance Tests in OSN.

Layer-stacked GO membranes were prepared by filtrating GO water suspension through a Nylon membrane substrate (Whatman, 0.2 μm pores). The GO membranes were dried thoroughly in a vacuum oven at 60 ℃ for 24 hours. To completely wet the GO membranes and achieve an equilibrate swelling, the GO membranes were soaked in the testing solvents for 12 hours before being tested. Solvent flux and rejection performance of the GO membranes were evaluated in a pressurized stainless-steel stir-cell. To achieve steady permeance and rejection ratio, GO membrane was first compressed under a high pressure of 70 psi for stabilization. Data were then collected under 50 psi. The concentrations of organic dye in feed, permeate, and retentate solutions were measured by using UV–vis spectrophotometer. The rejection R of markers was calculated using $R = \left(1 - \frac{C_p}{C_R}\right) * 100\%$, where C_p and C_R are the concentrations of markers in the permeate and retentate solutions, respectively.

REFERENCE

1. Li, H.; Song, Z.; Zhang, X.; Huang, Y.; Li, S.; Mao, Y.; Ploehn, H. J.; Bao, Y.; Yu, M., Ultrathin, molecular-sieving graphene oxide membranes for selective hydrogen separation. *Science* **2013,** *342* (6154), 95-98.
2. Kim, H. W.; Yoon, H. W.; Yoon, S.-M.; Yoo, B. M.; Ahn, B. K.; Cho, Y. H.; Shin, H. J.; Yang, H.; Paik, U.; Kwon, S.; Choi, J.-Y.; Park, H. B., Selective Gas Transport Through Few-Layered Graphene and Graphene Oxide Membranes. *Science* **2013,** *342* (6154), 91-95.
3. Hu, M.; Mi, B. X., Enabling Graphene Oxide Nanosheets as Water Separation Membranes. *Environ Sci Technol* **2013,** *47* (8), 3715-3723.
4. Huang, K.; Liu, G. P.; Lou, Y. Y.; Dong, Z. Y.; Shen, J.; Jin, W. Q., A Graphene Oxide Membrane with Highly Selective Molecular Separation of Aqueous Organic Solution. *Angew Chem Int Edit* **2014,** *53* (27), 6929-6932.
5. Sumboja, A.; Foo, C. Y.; Wang, X.; Lee, P. S., Large Areal Mass, Flexible and Free-Standing Reduced Graphene Oxide/Manganese Dioxide Paper for Asymmetric Supercapacitor Device. *Adv Mater* **2013,** *25* (20), 2809-2815.
6. Huang, J. Q.; Zhuang, T. Z.; Zhang, Q.; Peng, H. J.; Chen, C. M.; Wei, F., Permselective Graphene Oxide Membrane for Highly Stable and Anti-Self-Discharge Lithium-Sulfur Batteries. *ACS Nano* **2015,** *9* (3), 3002-3011.
7. Nair, R.; Wu, H.; Jayaram, P.; Grigorieva, I.; Geim, A., Unimpeded permeation of water through helium-leak–tight graphene-based membranes. *Science* **2012,** *335* (6067), 442-444.
8. Mi, B., Graphene oxide membranes for ionic and molecular sieving. *Science* **2014,** *343* (6172), 740–742.
9. Marchetti, P.; Solomon, M. F. J.; Szekely, G.; Livingston, A. G., Molecular Separation with Organic Solvent Nanofiltration: A Critical Review. *Chem Rev* **2014,** *114* (21), 10735-10806.
10. Huang, L.; Chen, J.; Gao, T. T.; Zhang, M.; Li, Y. R.; Dai, L. M.; Qu, L. T.; Shi, G. Q., Reduced Graphene Oxide Membranes for Ultrafast Organic Solvent Nanofi ltration. *Adv Mater* **2016,** *28* (39), 8669-8674.
11. Yang, Q.; Su, Y.; Chi, C.; Cherian, C. T.; Huang, K.; Kravets, V. G.; Wang, F. C.; Zhang, J. C.; Pratt, A.; Grigorenko, A. N.; Guinea, F.; Geim, A. K.; Nair, R. R., Ultrathin graphene-based membrane with precise molecular sieving and ultrafast solvent permeation. *Nat Mater* **2017,** *16* (12), 1198-+.
12. Li, W.; Wu, W.; Li, Z., Controlling interlayer spacing of graphene oxide membranes by external pressure regulation. *ACS Nano* **2018,** *12* (9), 9309-9317.
13. Zheng, S.; Tu, Q.; Urban, J. J.; Li, S.; Mi, B., Swelling of graphene oxide membranes in aqueous solution: characterization of interlayer spacing and insight into water transport mechanisms. *ACS Nano* **2017,** *11* (6), 6440-6450.
14. Joshi, R.; Carbone, P.; Wang, F. C.; Kravets, V. G.; Su, Y.; Grigorieva, I. V.; Wu, H.; Geim, A. K.; Nair, R. R., Precise and ultrafast molecular sieving through graphene oxide membranes. *Science* **2014,** *343* (6172), 752-754.
15. Szekely, G.; Jimenez-Solomon, M. F.; Marchetti, P.; Kim, J. F.; Livingston, A. G., Sustainability assessment of organic solvent nanofiltration: from fabrication to application. *Green Chem* **2014,** *16* (10), 4440-4473.
16. Talyzin, A. V.; Hausmaninger, T.; You, S.; Szabó, T., The structure of graphene oxide membranes in liquid water, ethanol and water–ethanol mixtures. *Nanoscale* **2014,** *6* (1), 272-281.

17. Wang, Z. Y.; Tu, Q. S.; Zheng, S. X.; Urban, J. J.; Li, S. F.; Mi, B. X., Understanding the Aqueous Stability and Filtration Capability of MoS_2 Membranes. *Nano Lett* **2017,** *17* (12), 7289-7298.
18. Wei, N.; Lv, C.; Xu, Z., Wetting of graphene oxide: A molecular dynamics study. *Langmuir* **2014,** *30* (12), 3572-3578.
19. Liu, R.; Arabale, G.; Kim, J.; Sun, K.; Lee, Y.; Ryu, C.; Lee, C., Graphene oxide membrane for liquid phase organic molecular separation. *Carbon* **2014,** *77*, 933-938.
20. Kim, J. E.; Han, T. H.; Lee, S. H.; Kim, J. Y.; Ahn, C. W.; Yun, J. M.; Kim, S. O., Graphene Oxide Liquid Crystals. *Angew Chem Int Edit* **2011,** *50* (13), 3043-3047.
21. Li, D.; Muller, M. B.; Gilje, S.; Kaner, R. B.; Wallace, G. G., Processable aqueous dispersions of graphene nanosheets. *Nat Nanotechnol* **2008,** *3* (2), 101-105.
22. Klechikov, A.; Yu, J.; Thomas, D.; Sharifi, T.; Talyzin, A. V., Structure of graphene oxide membranes in solvents and solutions. *Nanoscale* **2015,** *7* (37), 15374-15384.
23. Wei, N.; Peng, X. S.; Xu, Z. P., Understanding Water Permeation in Graphene Oxide Membranes. *Acs Appl Mater Inter* **2014,** *6* (8), 5877-5883.
24. Tsukahara, T.; Hibara, A.; Ikeda, Y.; Kitamori, T., NMR study of water molecules confined in extended nanospaces. *Angew Chem Int Edit* **2007,** *46* (7), 1180-1183.
25. Boukhvalov, D. W.; Katsnelson, M. I.; Son, Y. W., Origin of Anomalous Water Permeation through Graphene Oxide Membrane. *Nano Lett* **2013,** *13* (8), 3930-3935.
26. Huang, H. B.; Song, Z. G.; Wei, N.; Shi, L.; Mao, Y. Y.; Ying, Y. L.; Sun, L. W.; Xu, Z. P.; Peng, X. S., Ultrafast viscous water flow through nanostrand-channelled graphene oxide membranes. *Nat Commun* **2013,** *4*.
27. Jiao, S. P.; Zhou, K.; Wu, M. M.; Li, C.; Cao, X. L.; Zhang, L.; Xu, Z. P., Confined Structures and Selective Mass Transport of Organic Liquids in Graphene Nanochannels. *Acs Appl Mater Inter* **2018,** *10* (43), 37014-37022.
28. Hu, M.; Mi, B. X., Layer-by-layer assembly of graphene oxide membranes via electrostatic interaction. *J Membrane Sci* **2014,** *469*, 80-87.
29. Pines, E.; Fleming, G. R., Proton-Transfer in Mixed Water Organic-Solvent Solutions - Correlation between Rate, Equilibrium-Constant, and the Proton Free-Energy of Transfer. *J Phys Chem-Us* **1991,** *95* (25), 10448-10457.
30. Vanderhoeven, P. H. C.; Lyklema, J., Electrostatic Stabilization in Nonaqueous Media. *Adv Colloid Interfac* **1992,** *42*, 205-277.
31. Sarmini, K.; Kenndler, E., Ionization constants of weak acids and bases in organic solvents. *J Biochem Bioph Meth* **1999,** *38* (2), 123-137.
32. Vandezande, P.; Gevers, L. E. M.; Vankelecom, I. F. J., Solvent resistant nanofiltration: separating on a molecular level. *Chem Soc Rev* **2008,** *37* (2), 365-405.
33. Machado, D. R.; Hasson, D.; Semiat, R., Effect of solvent properties on permeate flow through nanofiltration membranes - Part II. Transport model. *J Membrane Sci* **2000,** *166* (1), 63-69.
34. Dikin, D. A.; Stankovich, S.; Zimney, E. J.; Piner, R. D.; Dommett, G. H. B.; Evmenenko, G.; Nguyen, S. T.; Ruoff, R. S., Preparation and characterization of graphene oxide paper. *Nature* **2007,** *448* (7152), 457-460.
35. Bacon, G. E., The Interlayer Spacing of Graphite. *Acta Crystallogr* **1951,** *4* (6), 558-561.
36. Bondi, A., Van Der Waals Volumes Radii. *J Phys Chem-Us* **1964,** *68* (3), 441.
37. Akbari, A.; Meragawi, S. E.; Martin, S. T.; Corry, B.; Shamsaei, E.; Easton, C. D.; Bhattacharyya, D.; Majumder, M., Solvent Transport Behavior of Shear Aligned Graphene Oxide

Membranes and Implications in Organic Solvent Nanofiltration. *ACS Appl Mater Inter* **2018,** *10* (2), 2067-2074.
38. Zheng, S. X.; Mi, B. X., Emerging investigators series: silica-crosslinked graphene oxide membrane and its unique capability in removing neutral organic molecules from water. *Environ Sci-Wat Res* **2016,** *2* (4), 717-725.
39. Marchetti, P.; Jimenez Solomon, M. F.; Szekely, G.; Livingston, A. G., Molecular separation with organic solvent nanofiltration: a critical review. *Chemical Reviews* **2014,** *114* (21), 10735-10806.
40. Tarleton, E. S.; Robinson, J. P.; Smith, S. J.; Na, J. J. W., New experimental measurements of solvent induced swelling in nanofiltration membranes. *J Membrane Sci* **2005,** *261* (1-2), 129-135.
41. Siffert, B.; Jada, A.; Letsango, J. E., Location of the Shear Plane in the Electric Double-Layer in an Organic Medium. *J Colloid Interf Sci* **1994,** *163* (2), 327-333.
42. Parsons, R., The electrical double layer in non-aqueous solvents. *Electrochimica Acta* **1976,** *21* (9), 681-686.
43. Murray, R.; Quirk, J., The Physical Swelling of Clays in Solvents 1. *Soil Science Society of America Journal* **1982,** *46* (4), 865-868.
44. Brown, K.; Thomas, J., A Mechanism by which Organic Liquids Increase the Hydraulic Conductivity of Compacted Clay Materials 1. *Soil Science Society of America Journal* **1987,** *51* (6), 1451-1459.
45. Chen, S.; Low, P. F.; Cushman, J. H.; Roth, C. B., Organic Compound Effects on Swelling and Flocculation of Upton Montmorillonite 1. *Soil Science Society of America Journal* **1987,** *51* (6), 1444-1450.
46. Brindley, G. W., Intracrystalline Swelling of Montmorillonites in Water-Dimethylsulfoxide Systems. *Clay Clay Miner* **1980,** *28* (5), 369-372.
47. Saiz, C. A.; Darvishmanesh, S.; Buekenhoudt, A.; Van der Bruggen, B., Shortcut applications of the Hansen Solubility Parameter for Organic Solvent Nanofiltration. *J Membrane Sci* **2018,** *546*, 120-127.
48. Mertens, M.; Van Goethem, C.; Thijs, M.; Koeckelberghs, G.; Vankelecom, I. F. J., Crosslinked PVDF-membranes for solvent resistant nanofiltration. *J Membrane Sci* **2018,** *566*, 223-230.
49. Postel, S.; Schneider, C.; Wessling, M., Solvent dependent solute solubility governs retention in silicone based organic solvent nanofiltration. *J Membrane Sci* **2016,** *497*, 47-54.
50. Graber, E. R.; Mingelgrin, U., Clay Swelling and Regular Solution Theory. *Environ Sci Technol* **1994,** *28* (13), 2360-2365.
51. Hildebrand, J. H., A History of Solution Theory. *Annu Rev Phys Chem* **1981,** *32*, 1-23.
52. Konios, D.; Stylianakis, M. M.; Stratakis, E.; Kymakis, E., Dispersion behaviour of graphene oxide and reduced graphene oxide. *J Colloid Interf Sci* **2014,** *430*, 108-112.
53. Boiadjiev, S. E.; Anstine, D. T.; Maverick, E.; Lightner, D. A., Hydrogen-Bonding and Pi-Stacking in Dipyrrinone Acid Dimers of Xanthobilirubic Acid and Chiral Analogs. *Tetrahedron-Asymmetr* **1995,** *6* (9), 2253-2270.
54. Wei, S. C.; Xie, Y.; Xing, Y. D.; Wang, L. C.; Ye, H. Q.; Xiong, X.; Wang, S.; Han, K., Two-dimensional graphene Oxide/MXene composite lamellar membranes for efficient solvent permeation and molecular separation. *J Membrane Sci* **2019,** *582*, 414-422.

55. Guo, B. Y.; Jiang, S. D.; Tang, M. J.; Li, K. R.; Sun, S. P.; Chen, P. Y.; Zhang, S., MoS2 Membranes for Organic Solvent Nanofiltration: Stability and Structural Control. *J Phys Chem Lett* **2019,** *10* (16), 4609-4617.
56. Mi, B. X.; Zheng, S. X.; Tu, Q. S., 2D graphene oxide channel for water transport. *Faraday Discuss* **2018,** *209*, 329-340.
57. Wang, J. W.; Dlamini, D. S.; Mishra, A. K.; Pendergast, M. T. M.; Wong, M. C. Y.; Mamba, B. B.; Freger, V.; Verliefde, A. R. D.; Hoek, E. M. V., A critical review of transport through osmotic membranes. *J Membrane Sci* **2014,** *454*, 516-537.